Remote Sensing Applications: Society and Environment 15 (2019) 100233

Contents lists available at ScienceDirect

Remote Sensing Applications: Society and Environment

journal homepage: www.elsevier.com/locate/rsase

Assessing land use/cover dynamics and exploring drivers in the Amazon's arc of deforestation through a hierarchical, multi-scale and multi-temporal classification approach

Andrea S. Garcia[a,b,*], Vívian M. de F. N. Vilela[a], Rodnei Rizzo[a], Paul West[b], James S. Gerber[b], Peder M. Engstrom[b], Maria Victoria R. Ballester[a]

[a] Center for Nuclear Energy in Agriculture, University of São Paulo, Piracicaba, Brazil, CENA/USP
[b] Institute on the Environment, University of Minnesota, Saint Paul, Minnesota, USA, IonE/UMN

ARTICLE INFO

Keywords:
Land use change
Amazon
Cerrado
Ecotone
Physiognomies

ABSTRACT

Land use and land cover (LULC) are intrinsically tied to ecological and social dynamics. Still, classifying LULC in ecotones, where landscapes are commonly heterogeneous and have a wide range of physiognomies, remains a challenge. Here we present a three-level hierarchical classification approach, using both Landsat and MODIS images, and both pixels and objects as units of information. We applied this multi-temporal and -spatial approach to classify land use in the Upper Xingu River Basin (~170,000 km^2), located in the arc of deforestation of the Brazilian Amazon. The first level includes five classes and differentiates managed land from native vegetation with high overall accuracy (93%). The second level has 11 classes (overall accuracy = 86%) and separates main land uses and native vegetation domains. The third level has 16 classes (overall accuracy = 83%) and addresses productivity of both managed and natural systems. We find that this new method presented here is more efficient than existing regional and global land cover products. Applying this approach to assess land cover transitions in the basin from 1985 to 2015, we find that agricultural production increased, yet manifested itself differently in the northern (Amazon biome) and southern (Cerrado biome) portions of the basin. Analyzing land use change in different levels, we identify that agricultural intensification occurred mainly in the Amazon while the Cerrado has undergone an expansion in agricultural area. The method presented here can be adapted to other regions, improving efficiency and accuracy of classifying land cover in heterogeneous landscapes.

1. Introduction

Land cover refers to the observed biophysical component on the Earth's surface, while land use is defined by the activities undertaken in a certain area (Di Gregorio, 2016; Turner et al., 2007). Land use and land cover (LULC) changes are key components of biological, physical, and socioeconomic processes taking place on the Earth surface (de Chazal and Rounsevell, 2009; Don et al., 2011; Foley et al., 2005; Lathuillière et al., 2017; Macedo et al., 2013). Therefore, LULC is a fundamental input for several models in many research areas and can help inform decision making processes (Bondeau et al., 2007; Döll et al., 2003; FAO, 2011, 1993; Ge et al., 2007). Remotely sensed products are the main data source for LULC mapping, and much research has been devoted to evaluating methodologies with a specific emphasis on classification techniques (Coppin et al., 2004; Gómez et al., 2016; Hansen and Loveland, 2012; Hussain et al., 2013; Tewkesbury et al., 2015; Wang et al., 2017). Despite the large efforts and achievements in improving LULC classification, accurately transforming remotely sensed data into thematic maps remains a challenge when modelling complex landscapes (Gómez et al., 2016), limiting our ability to address patterns and processes of LULC change, especially in tropical regions (Müller et al., 2015; Pendrill and Persson, 2017; Toniol et al., 2017).

Ecotones, agriculture frontiers and biomes with multiple physiognomies present large disagreement in global and continental datasets (Giri et al., 2005; Herold et al., 2008; Pendrill and Persson, 2017). For example, Herold et al. (2008) identified that at least three out of four global data sets disagree on LULC classes attributed to large portions of the Amazon's Arc of Deforestation and neotropical savanna biomes. Factors that contribute to this disagreement are associated with the large biophysical variability observed in diverse landscapes. Inadequately assessing the spatial and temporal

* Corresponding author. Lab. Geoprocessamento, Centro de Energia Nuclear na Agricultura , Universidade de São Paulo, Av. Centenário, 303, 13400-970, Piracicaba, SP, Brasil.
E-mail address: andreagarcia@usp.br (A. S. Garcia).

https://doi.org/10.1016/j.rsase.2019.05.002
Received 23 January 2019; Received in revised form 30 April 2019; Accepted 1 May 2019
Available online 13 May 2019

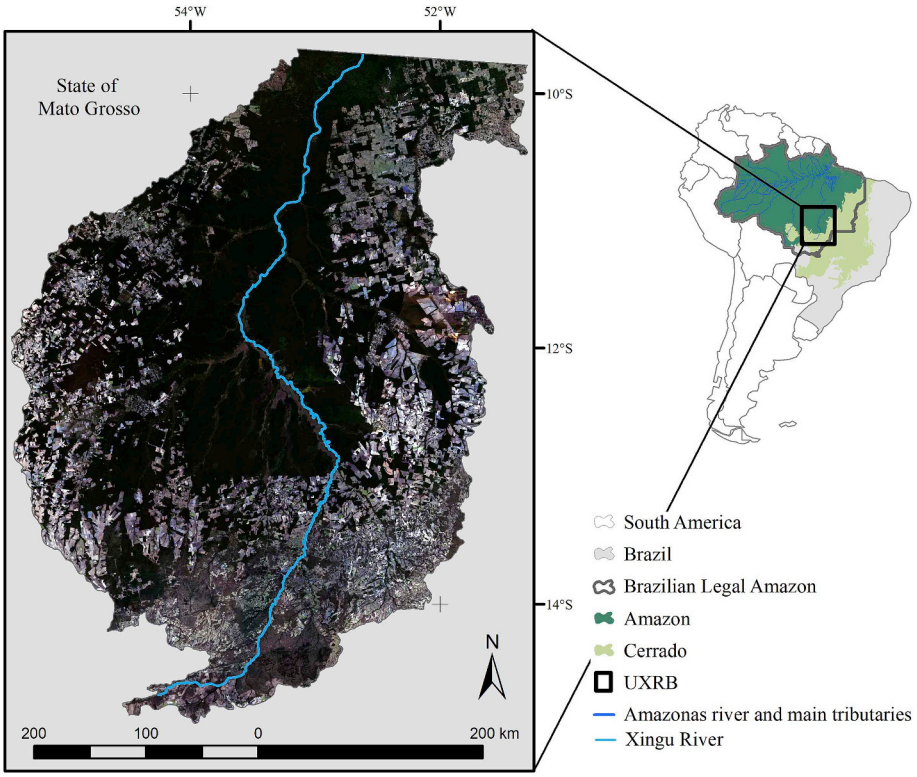

Fig. 1. Upper Xingu River Basin (UXRB) is located in the Brazilian Legal Amazon, state of Mato Grosso. It drains an area of ~170,000 km^2 into the Xingu River, one of the main tributaries of the Amazonas River. The area is in the ecotone between the Amazon and Cerrado biome (also known as neotropical savannas). The image on the left is a mosaic of Landsat 8 images acquired in July and August of 2015. The mosaic is shown in a true-color composition (RGB 432).

variability of these areas precludes the possibility of adequately capturing their LULC classes. Additionally, accuracy of LULC maps generally decreases with increasing class complexity (Lu and Weng, 2007), which is very often important for decision-making. Still, improving LULC monitoring is critical to evaluating impacts on the extent, condition, and productivity of both managed and natural systems. Such dynamics are directly linked to several social or ecosystem services, including food, water and energy security, and biodiversity conservation (Endo et al., 2015 > ; Lal, 2016; Ozturk, 2015). This information is essential when planning land use in regions such as the neotropical savannas (*Cerrado*) or the tropical rainforest at the Amazon's arc of deforestation. These regions are not only hotspots for biodiversity conservation, but are also undergoing rapid LULC change due to agriculture expansion (Klink and Machado, 2005; Power, 2010). Aside from the importance of these regions in terms of natural resources and agricultural production, spatially explicit LULC information that considers landscape diversity is rarely available.

Classification techniques refer to the process of sorting pixels into a finite number of individual classes, based on their surface reflectance values at a certain time (Lu et al., 2004), or the reflectance behavior of pixels through time (e.g.: MODIS Land Cover products (Friedl et al., 2010)). Use of both high spatial and temporal resolution data is an approach that increases both the amount of data and the modelling complexity, while enabling the study of different native vegetation physiognomies or agriculture productivity (Brown et al., 2007; Ferreira et al., 2003). Due to increases in modelling complexity, current products address either spatial or temporal resolution when classifying LULC. The computational challenge of modelling large satellite imagery data sets can be made more efficient using an object-based approach (Blaschke, 2010). But this approach is not appropriate for landscape formations which are not expected to present a spectral pattern of an object (a group of pixels presenting a similar response). Still, for small scale study areas, approaches that integrate pixel-based and object-based methods out-perform approaches that employ only one of these methods on their own (Aguirre-Gutiérrez et al., 2012; Chen et al., 2018). Recently, the combination of machine (or deep) learning, cloud processing, and big data is shifting classification processing by enabling users to address more complex models of classification (Azzari and Lobell, 2017); mainly when the physical processes resulting in the remotely sensed imagery are not understood, or are not the main focus of the study (Zhu et al., 2017). Such data-driven classifications rely on many redundant explanatory variables (Lebourgeois et al., 2017), and results often are not easily translated into a conceptual model. In this regard, Zhu et al. (2017) argue that uniting process-based modelling and machine learning is a promising direction.

Here we present a hierarchical classification approach which applies a multi-temporal/multi-scale and combined object and pixel-based approach in order to contribute to diverse landscape LULC mapping. We demonstrate that through this approach we improve the assessment of LULC change patterns and their causation chains. Moreover, this study is intended to improve classification processes by presenting a workflow which (i) generates a classification allowing the analysis of LULC change in modern agricultural frontiers and ecotone zones, (ii) facilitates the comparison of results with those generated by other studies and/or for other regions, (iii) uses freely available remote sensing data, and (iv) employs a straightforward approach that can be implemented in software commonly used and/or available at no cost to researchers, NGOs, and governmental agencies (R, GRASS, or Orpheum toolbox). We tested this approach by creating a series of multi-temporal LULC maps for the Upper Xingu River Basin, located at the border of the Amazon rainforest and neo-tropical savannas (*Cerrado*), and describing the changes over three decades. We then explore patterns, trajectories, and causes of LULC change for this study area.

2. Study area and data

2.1. Study area

The Upper Xingu River Basin (hereafter denoted as “UXRB”), is located in Mato Grosso state in Brazil, and in the ecotone between the Amazon rainforest and the neotropical savannas, or Cerrado biome. The Xingu River is one of the main Amazon River tributaries. Its headwater region encompasses one-third of the Xingu River Basin, draining ~170,000 km^2. The area spreads from about 9.5°S to 15°S and from 51°W to 55.5°W (Fig. 1). The UXRB exhibits a wide array of natural physiognomies, ranging from Amazon rainforest to savanna grasslands (Ivanauskas et al., 2008; Velasquez et al., 2010). The Amazon rainforest

and Cerrado are the first and second largest biomes in South America. The Amazon rainforest contains enormous biodiversity and one-third of the world's tropical tree species used for timber (Brasil, 2018). The Cerrado is a global biodiversity hotspot and contains the highest land use change rates in Brazil (Brasil, 2018; Klink and Machado, 2005).

Besides the importance of the region for its natural resources (including biodiversity), the UXRB also encompasses large sociocultural diversity and economic prominence. It is estimated that 16 indigenous ethnic groups and other traditional communities live in the basin (Velasquez et al., 2010). The main economic activities in the study area during the late 1970's to 1990's were timber and beef. Forests were degraded or cleared due to livestock expansion and logging activities. In the early 2000's, soybean production emerged as another deforestation driver (Brando et al., 2013; Nepstad et al., 2006). The defined rainy season, flat terrain, and dominance of good physical structured Oxisol soils (Velasquez et al., 2010), make the UXRB ideal for agricultural expansion and intensification. Currently, approximately 2% of world's and 9% of Brazil's soybeans are produced in the UXRB, as well as 0.2% of the world's and 13% of Brazil's cattle (FAOSTAT, 2016; IBGE, 2016).

2.2. Data acquisition and pre-processing

LULC maps for 1985, 1990, 1995, 2000, 2005, 2010, and 2015 of the UXRB were derived from a combination of Landsat (L5, L7 or L8, level 2) and MODIS (Aqua and Terra, collection 6) products. These images were processed based on information gathered through the Brazilian vegetation map (IBGE, 2004), ground reference points, and fine resolution images (Rapideye).

2.2.1. Landsat data

Landsat surface reflectance images were obtained from the USGS/Landsat Higher Level Science Data products (http://espa.cr.usgs.gov/). The path/row and acquisition date of all 120 Landsat scenes used in this study are presented in Supplementary Material 1. Landsat Higher Level Science Data products are delivered pre-corrected for geometrically and radiometrically by a homogenous correction chain (Masek et al., 2006; http://espa.cr.usgs.gov/). Although previously corrected, we registered mosaicked and resampled (30 m pixel resolution) images by using autosync workstation (ERDAS, 2014a) in order to guarantee a pixel by pixel overlap between years. As the UXRB presents a flat relief, we implemented a 2D polynomial model of third order based on the green band of each image. We considered 15 m, half pixel resolution, as the maximum acceptable error value (Root Mean Square Error < 0.5 pixel) and resampled the images through cubic convolutions. This process was particularly important for earlier years, as shown in Supplementary Material 1. A histogram matching procedure was applied when necessary during mosaicking processes based on central path (225 in the WRS-2 system) overlapping areas. Since all raster in the time series share a similar histogram shape, this technique changes each of the pixel's values according to the target histogram but does not change the histogram shape.

No radiometric correction was applied with the exception of Landsat 7 images for 2005 and 2010 which were striped - images collected after 2003, when the Scan Line Corrector (SLC) failed. To correct this error, we applied a gap filling technique, which consists on acquiring a second image (also from Landsat 7 and for same year as the original one) to fill the gaps in the first scene (Scaramuzza et al., 2004). Rather than using these corrected images as primary sources of data to build LULC maps, we used them to visually verify Landsat 5 image consistency. Since Landsat 5 was launched in 1984, and old sensors can present degradation problems in more recent acquisitions. We did not use any image with signs of degradation.

2.2.2. MODIS and derived indices

MODIS Enhanced Vegetation Index (EVI), with a 250 m spatial resolution and 8 day temporal resolution were acquired on demand from the University of Natural Resources and Life Sciences, Vienna - BOKU (Vuolo et al., 2012). This database is based on MODIS Level-3, 16-day composite EVI from both Terra and Aqua satellites. The combination of 16-day composites from both satellites allowed us to derive a time series of 8-day temporal resolution. EVI time-series are delivered mosaicked, smoothed, and gap-filled. Such processing steps are based on the "MODIS package" (Mattiuzzi et al., 2016) developed in *R* (R Development Core Team, 2011), and the Whittaker filter (Vuolo et al., 2012). We tested EVI images against our Landsat mosaic using the previously described process, but no geometric correction was needed. An annual EVI series beginning in August of each analyzed year and ending in August of the following one was built for 2000, 2005, 2010 and 2015. In total, we used 832 MODIS scenes, or ~210 for each year.

2.2.3. Ground reference

We carried out field work to collect ~2000 ground reference points in two independent campaigns. The first campaign, carried out in June 2015, was used to improve systematic comprehension of the study area's LULC composition and to create thresholds for LULC class separability criteria. This dataset is composed of ~400 ground reference points collected on the ground. In addition, ancillary reference data points (~100 points) were collected by comparing Landsat 8 images obtained in 2015 with high spatial resolution RapidEye images acquired in 2012/13 (http://geocatalogo.mma.gov.br/). Hereafter this dataset is called "training data" and its overview is presented in Supplementary Material 2. The field work to develop the training data was mostly concentrated at the contact zone between tropical rainforest and savannas, as well as at areas with more intense land use change.

During a second campaign (October 2016), we acquired 1500 ground reference points throughout the entire basin for accuracy analyses. The points were as distributed in the basin as practical, but concentration around the main roads was inevitable due to access constrains and study area size. In addition, an ancillary set of data points (~500 points) collected by an independent researcher though a comparison of Landsat 8 images of the year 2016 with RapidEye images was also used. This complementary approach was necessary in order to sample large areas which are difficult to assess. This dataset, hereafter called "validation data", was used to verify the quality of the final classification.

3. Methods

To derive LULC maps in highly dynamic tropical ecotone zones, we developed an assessment approach through a hierarchical classification model which allows us (i) to assess relevant information for regional landscape evaluation, (ii) to have different levels of information and accuracy for a diverse range of applications, (iii) to harmonize our thematic mapping with LULC schemes produced for other tropical regions or globally, and (iv) to apply the same classification methodology in other study areas. The hierarchical classification model was built in ERDAS Imagine Expert Classifier workstation (ERDAS, 2014b). We applied a hierarchical rule-based approach (a decision tree based on expert knowledge) to integrate variables of different sources and formats. Each branch describes the conditions under which constituent information (variables) gets abstracted into a set of higher-level informational classes. The rules were set based on literature and expert information, and field work observation. This approach focuses on expected reflectance signals based on knowledge of LULC behavior though space and time. It differs from currently popular machine learning algorithms, which fish a signal from data through multiple variable interactions (Maxwell et al., 2018). The development of classifications we applied here advances variable selection based on patterns and process behavior concepts, and can be used in any kind of classification, including machine learning. It is also important to note that learning algorithms demand a large and well distributed field sample to train the algorithms, which still is not always the case for

Table 1
Description of the land cover and land use classes used in this study. Level refers to the hierarchical level in the classification scheme.

Level	Class	Description
1	Natural and semi-natural vegetation	Natural or semi-natural vegetation cover, including forest, savannas, and floodplains
	Cultivated and managed terrestrial areas	Any area under management which modifies the physiognomy of a natural system
1	Burned areas	Either natural or managed areas that have recently being burned
2	Surface water	Area covered by water
3	Unclassified	Any pixel that did not fit in any of the other categories
2	Forest	Forest formations, including rain forest, semi-deciduous, deciduous, riverine, cerradão (cerrado woodland with closed canopy)
	Savanna formation	Wood-grassland ecosystem with open canopy
	Croplands	Cultivated areas
	Pasturelands	Areas with planted grassland for cattle ranching
2	Wetlands	Flooded area, either permanently or seasonally with high proportion of vegetation.
3	Secondary complex	Vegetation in regeneration or disturbed through natural processes or removal
	Bare soils	Exposed bare soil lacking any vegetation
	Urban	Concentrated built-up structures
3	Forest	Forest formations in the Amazon domain such as rain and deciduous forests
	Forest cerrado	Forest formations in the Cerrado domain such riparian forest and woodland
	Woody Cerrado	Woody formation with open canopy and at least 40% of tree cover
	Shrub-grassland cerrado	Grassland formation with no trees to formations with up to 40% of tree cover
	Single crop	Cultivated areas with one harvest per year, rain fed
	Double crop	Cultivated areas with two harvests per year, rain fed
	Irrigated crop	Cultivated areas which are artificially irrigated
	Pasturelands	Areas with regular planted grassland for cattle ranching
	Degraded pasturelands	Areas with planted grassland for cattle ranching with presence of bare ground and poor greenness recovery

extensive tropical areas. Still, a preliminary classification as we apply here could contribute with sample allocation to develop even more powerful classification processes.

Legend can be defined as the application of a classification scheme in a specific study area. Here we used three levels of information to address LULC legend, each level composed for both land cover classes and land use classes. We considered representative LULC classes for the ecotone zone between Amazon rainforest and Cerrado both in area and in meaning of LULC change. The border between both biomes extends for about 6300 km and overlaps with the Amazon's arc of deforestation. The developed LULC legend follows hierarchical concepts presented by FAO's Land Cover Classification System (Di Gregorio and Jansen, 2000). First, we adopted a general level of information on LULC, followed by a differentiation of the main land use and native vegetation domains. The third level of classification is linked to productivity and addresses land use intensity as well different native physiognomies. It is important to point out that we do not differentiate all 11 savanna vegetation physiognomies, which range from forest to grassland fields with no trees (see Oliveira and Marquis (2002) for further description). Instead, we aggregated them into three different classes according to tree density. Previous global (GLC2000 (Bartholomé and Belward, 2005) and MODIS Global land cover (Friedl et al., 2010)), and regional (TerraClass Cerrado (Scaramuzza et al., 2017) and TerraClass Amazonia (Almeida et al., 2016)) efforts produced legends compatible with our intermediate classification level, but no more detailed information on productivity systems or physiognomies are provided.

The spatial-temporal resolution of the final classification products is also of high interest when assessing LULC change. Here we took advantage of Landsat spatial resolution (30 × 30 m) and EVI MODIS temporal resolution (7 days) by combining both products and addressing LULC change in terms of cover and management. EVI MODIS time series presents a 250 m spatial resolution, moreover to overcome this problem, we segmented Landsat images and used the derived objects (larger than 250 m) to extract data from EVI MODIS layers by calculating the modal (discrete variables) or mean value (continuous variables) of pixels contained in each object. This approach is referred to as “zonal” in following sections. Level 1 and level 2 products are made available for each 5-year period from 1985 to 2015. Level 3 was only developed for 2000–2015 due to MODIS availability. Nevertheless, the employment of both Landsat and MODIS sensors allows us to rely on the spatial resolution of the former and the temporal resolution of the latter to address mainly the Level 3 of our classification.

3.1. Decision tree and classification rules

Our hierarchical classification model consisted of three levels as presented in Table 1. Level 1 (L1) classifies the region of interest into five major LULC types: (1) natural and semi-natural vegetation, (2) cultivated and managed terrestrial areas, (3) burned areas, (4) surface water, and (5) unclassified (see Fig. 2 for decision tree overview). This legend is fairly comprehensive and can be harmonized with a broad range of other researches, reducing conversion uncertainties among different products. L1 assesses native vegetation conversion and, thus, supplies information for policies and laws, such as the Brazilian Forest Code (Soares-Filho et al., 2014). To develop this level, first, we applied an unsupervised classification method using ISODATA algorithm to classify Landsat mosaicked images. In this process, each pixel is assigned to a class based on its spectral profile. There is no need for prior knowledge of the number or identification of the different classes present in the imaged area. We set the ISODATA algorithm to cluster pixels in up to 40 classes based on up to 20 iterations, with a minimum size of 0.01% of the study area for each class, a maximum standard deviation of 5, a maximum of 2 merges, and a convergence threshold of 0.95. Finally, we visually aggregated each of the output classes into one of the five legend classes mentioned before.

Level 2 (L2) encompasses a more specific set of LULC classes, but is broad enough to be adapted or compared to similar regions throughout the tropics. This legend level assesses biophysical characteristics related to LULC of the target landscape. For example, L2 is useful as an input for biogeochemical and hydrological models as it differentiates vegetation types. LULC information and user's knowledge acquired in field work was necessary to map LULC at the second level of detail (see Fig. 2 for decision tree overview). LULC legend for the L2 included: (1) forest (2) savanna formation (3) wetlands (4) secondary complex, (5) croplands, (6) pasturelands, (7) bare soils, (8) urban, (9) burned areas, (10) surface water, and (11) unclassified. L1 unsupervised classification output was disaggregated into forest (closed canopy), savanna formation (open canopy), wetlands, and secondary complex. We disaggregated these classes by overlapping the Brazilian Institute of Geography and Statistics vegetation map as a masking conditional variable, with the classes resulting from the unsupervised classification (described above) being classified as Natural/Semi-natural (L1). Areas

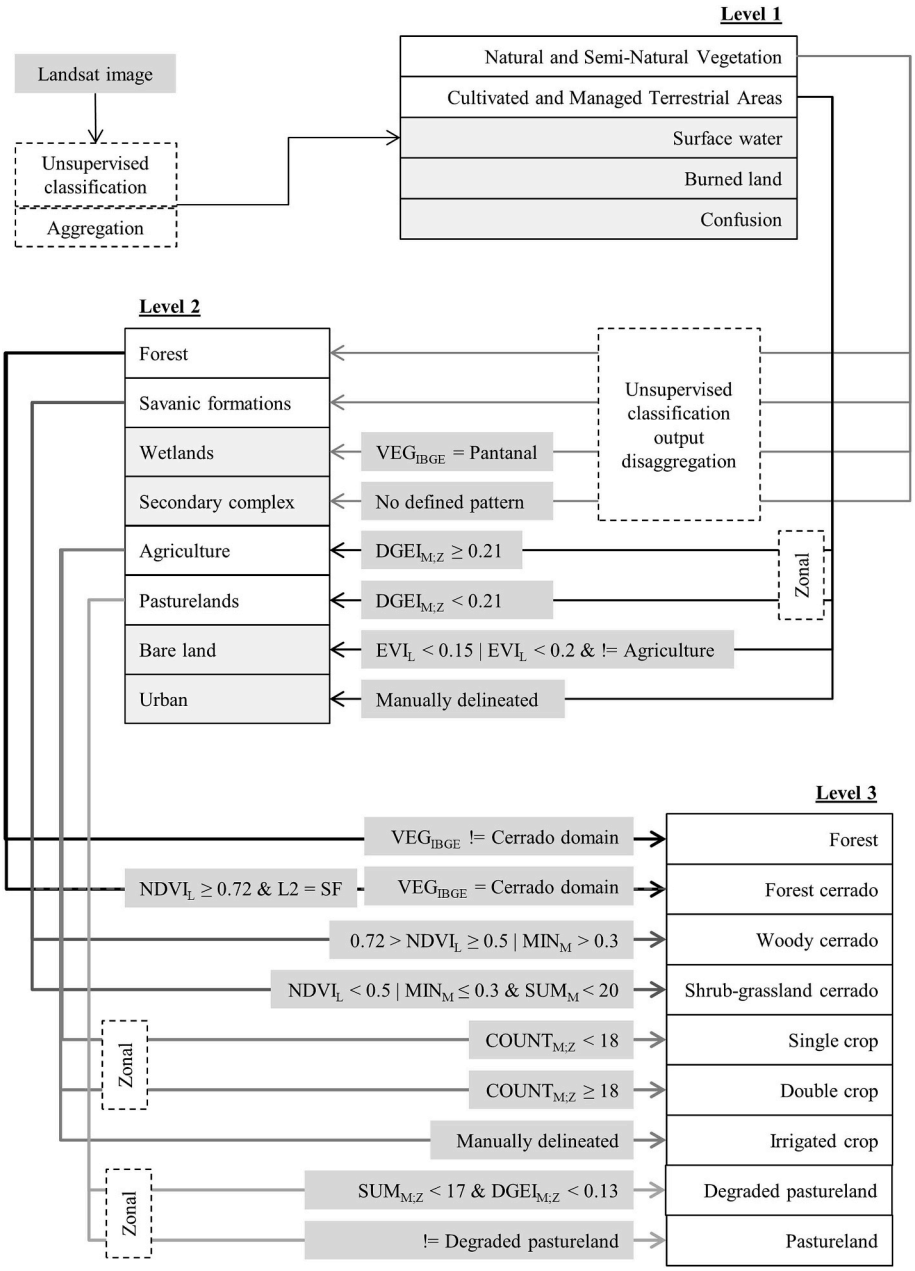

Fig. 2. Workflow of the three-level hierarchical classification system developed and applied to derive a 30-year time series of land use and land cover maps of the UXRB, Brazil. Grey boxes indicate the data used in each decision rule designed to obtain a certain class. Solid line boxes represent land use and land cover classes. Land use and land cover classes boxes highlighted in light grey are classes that are carried over to next level of classification without modification. Whenever a class is derived based on an object approach, the arrow defining the respective workflow pass by a "zonal" box delimited by dotted lines. All thresholds presented here were developed for the study area only and can be used as approximate values for similar regions.

where both maps did not match were considered secondary complexes. Urban, burned areas and surface water were imported from L1 without any modification. Forest, savanna, urban, burned areas and surface water formation were inputted in L2 classification based on pixel since we do not expect them to necessarily present object patterns.

We segmented Landsat images to reclassify managed areas. Segmentation was conducted in ArcGIS 10.3 using bands 5, 6, and 4 of mosaicked Landsat 8 images (bands 4, 5, and 3 for years using Landsat 5 or Landsat 7) based on the spectral similarity and spatial proximity among neighbor pixels, with a minimal area of 9 ha. This approach assumes a minimal aggregated number of pixels or a specific shape in crops and pasturelands. We arbitrary chose a minimum area of 9 ha with the goal of adding variance to the analyses but also allowing the algorithm to capture the smallest area as possible. We chose 9 ha so we could evaluate more than one Modis' pixel (pixel resolution equal to 250 m, resampled into 30 m, and resulting in ~70 pixels), and 100 Landsat pixels (pixel resolution equal to 30 m). We classified each object according to L1 classes by defining the major class inside each object and identified Managed Areas which were then reclassified in crops, pasturelands or bare soils. To differentiate these three classes based on MODIS EVI, we calculated three indexes based in relation to the agriculture calendar for Mato Grosso state (Supplementary Material 3). We used the objects created with Landsat images to calculate the mean value for each object (referred to in Fig. 2 as zonal approach) and each index. Indexes based on MODIS EVI are as follow:

(Index i) Minimum EVI during soil preparation/sowing season (EVImin)

$$EVI_{min} = MIN\,(EVI_{so(doy\,x)},\ EVI_{so(doy\,x+7)},\ldots,EVI_{so(day\,y)})$$

where:

EVI_{so} series represents a sequence with 7-day interval from the first day (doy x) of the soil preparation/sowing season to the last one (*doy y*), *doy* corresponds to day of the year in the julian calendar;

(Index ii) Maximum EVI in the growing season (EVI_{max})

$$EVI_{max} = MAX\,(EVI_{gro(doy\,x)},\ EVI_{gro(doy\,x+7)},\ldots,EVI_{gro(doy\,y)})$$

where.

EVI_{gro} series represents a sequence with 7-day interval from the first day (*doy x*) of the growing season to the last one (*doy y*);

(Index iii) Differential greenness enhancement index (Rizzi et al., 2009)

$$DGEI = \frac{EVI_{max} - EVI_{min}}{EVI_{max} + EVI_{min}}.$$

We assumed that crop areas presented both states: bare soil or haystacks due to soil preparation and sowing period (very low EVI values), and also at least one green period during a year due to the growing season (highest EVI values). Moreover, they presented a higher DGEI when compared to pasturelands. As DGEI is the contrast between the peak high and low values of EVI in a season (defined as a few months), it is not sensitive to normal seasonality and precipitation shifts. Still, it can potentially be affected by drastic droughts which negatively impact both crop and pasture growth. Additionally, cropland abandonments can potentially impact this index. Such dynamics prevent land covers from reaching their expected maximum or minimum EVI values. Optimal DGEI thresholds values were identified based on training sampled data. However, since EVI time-series from MODIS are available after 2000, we applied other methods to separate crops from pastures for 1985, 1990 and 1995. For these years, we identified cropland polygons by selecting objects which presented Landsat EVI values lower than 0.3 (bare soil or stover – based on visual selection of sample fields which remained unchanged between 1995 and 2000, and were classified as croplands in 2000) and minimum field size of 40 ha. Cropland area is certainly under estimated for those dates. However, as croplands account for a maximum of 1% of the UXRB basin before 1995 (IBGE, 2016), we trust this procedure did not compromise our results.

The main goal of Level 3 (L3) is to cope with ecological characteristics related to LULC such as regional agriculture greenness or ecological intensification (Arvor et al., 2012). It is also useful, for example, when analyzing socio-economic characteristics associated with crop and cattle ranching intensification or to analyze which natural physiognomies are more likely to be replaced by certain agricultural activity (see Fig. 2 for decision tree overview). LULC legend for L3 included: (1) forest, (2) forest cerrado, (3) woody Cerrado, (4) shrub-grassland cerrado, (5) wetland, (6) secondary complex, (7) single crop, (8) double crop, (9) irrigated crop, (10) pasturelands, (11) degraded pasturelands, (12) bare soils, (13) urban, (14) burned areas, (15) surface water, and (16) unclassified. L3 maps include classes that rely on high resolution temporal images, available only from 2000 forwards due to MODIS availability. We identified low productivity pasturelands (or degraded pasturelands) by using a combination of two indices derived from MODIS EVI: annual EVI_{sum} and annual DGEI.

(Index iv) Sum of EVI in a certain year (EVI_{sum})

$$EVI_{sum} = \sum (EVI_{gro(doy\ x)}, EVI_{gro(doy\ x+7)}, \ldots, EVI_{gro(doy\ y)})$$

where EVI_{sum} series represents a sequence with 7-day interval from the first day (*doy x*) of the analyzed period through the last one (*doy y*).

The applied analysis adopts the hysteresis principle, which means that degraded pasturelands present a lower resilience and, thus, they are not able to recover their original state after a disturbance period (Searle et al., 2009; Yengoh et al., 2015). Grazing, fire, and water shortages are forms of disturbance, and the lack of recovery implies a loss of pasture productivity. This loss is liked to biological degradation (decrease in carbon accumulation) but also with some agricultural degradation processes such as loss of productivity in the form of insect attacks, for example (Dias-Filho, 2001). DGEI calculated as shown previously based on the whole analyzed year was used to estimate how recovering photosynthetic capacity varied within a year. The cumulative vegetation index (EVI_{sum}) was used as a proxy for net primary productivity (Ferreira et al., 2013). We considered the combination of low greenness and low annual variation as indicative of pasturelands in degradation. Both DGEI and EVI_{sum} were used to include the temporal EVI variation associated to rainfall (Yengoh et al., 2015). Although this approach does not addresses the complexities of the pasture degradation process, it is a fair indicator of pasture resilience through different seasons (Yengoh et al., 2015). Croplands were reclassified according to a conditional model of double cropping detection. Whenever croplands presented a large number of days with high vegetative response, we consider them as double cropping areas as shown in the following formula:

(v) Count of days with EVI $>$ 0.5 in a certain year (EVI_{count})

$$EVI_{count} = \sum (EVI_{veg,doy\ x}, \ldots, EVI_{veg,\ doy\ y})$$

$$EVI_{veg,doy\ x} = 1 \rightarrow EVI_{doy} > 0.5$$

$$EVI_{veg,doy\ x} = 0 \rightarrow EVI_{doy} \leq 0.5$$

Where EVI_{veg} represents a sequence with 7-day interval from the first day (doy x) of the analyzed period through the last one (doy y). Each EVI_{veg} is assigned the value 1 if the correspondent EVI value at certain day is higher than 0.5, otherwise it is zero. Irrigated areas were manually extracted based on spatial arrangement and higher EVI reflectance in the dry season. The optimal thresholds were calculated based on the training sample data.

We used the Brazilian vegetation map (IBGE, 2004) to first break forest areas into forest (L2-forest inside the rain forest domain) and forest cerrado (L2-forest inside the savanic domain). We also relied on NDVI values calculated from Landsat images in the dry season ($NDVI_L$), and EVI_{min}, and EVI_{sum} values to reclassify forest and savanic formations into forest, forest cerrado, woody Cerrado, and shrub-grassland cerrado. The optimal thresholds were also calculated based on the training sample data - they are shown in Fig. 2.

3.2. Accuracy assessment

We produced a confusion matrix based on (i) reference points collected in 2016 on the ground (total of 1460 ground reference points), and (ii) reference points collected through very high-resolution Rapid Eye images from 2012 to 2013 (total of 489). We transformed the observed sample confusion matrix into an estimated population matrix, as recommended by Pontius et al., (2011). Then, we calculated overall (dis)agreement, overall quantity disagreement (amount of disagreement due to the quantity of each class), and overall allocation disagreement (amount of disagreement due to the miss-overlap of classes in space). Disagreement and its decomposition were also calculated for classes. Further details on accuracy assessment are available in Supplementary Material 4. As accuracy metrics calculated directly from the observed sample confusion matrix are still very common in the literature, we also present these metrics in Supplementary Material 4.

Once the classification process for the 2015 images returned a satisfactory output, we assumed that the analyst acquired the “know how” of the classification process, and could classify previous years using the same rules. In the process, we visually checked whether different thresholds would improve the classification of sample points with a marked land cover, but no improvement was observed. We did not collected data to estimate accuracy for previous year. But we assumed the 2015 accuracy assessment would also apply for previous year. It's important to point out that burned lands were not considered in such analysis. Burned lands class is present in a short temporal window, which makes it almost impossible to collect ground reference points. Thus, it was omitted from analyses. Still, such class presents a very distinct spectral profile and, then, it would not significantly change the accuracy results. A detailed explanation of reference data collection and analyses is showed in Supplementary Material 4.

In addition to the validation database collected in our field surveys, we used LULC information from Amazon Environmental Research

Table 2
Overall agreement, quantity disagreement, allocation disagreement, and number of classes relative to the proposed land use and land cover classification workflow in the Upper Xingu River Basin (Mato Grosso, Brazil) in 3 levels of information. Calculation was based on comparison with 1500 ground reference points collected in 2016. Complete error matrix can be assessed in Supplementary Material 4.

Reference database (2016)			
	Level 1	Level 2	Level 3
Overall agreement (%)	93.21	86.49	83.64
Quantity disagreement (%)	4.43	8.84	10.19
Allocation disagreement (%)	2.35	4.67	6.17
N° of classes	5	11	16

Institute (IPAM, http://ipam.org.br), Socio-Environmental Institute (ISA, https://www.socioambiental.org) and The Brazilian Institute of Geography and Statistics (IBGE, 2016) to evaluate our results in separate analysis. The IPAM database includes LULC ground reference points obtained in 2017 for Querência municipality. ISA database contains maps for multiple years of LULC for Querência, Canarana, São José do Xingu, and Santa Cruz do Xingu municipalities, which in turn represent together about 25% of the UXRB. We randomly sampled these maps and compared each point with the ones from our output maps for the 2010 and 2015 years. ISA's and IPAM's LULC information were not as detailed as our L3 classification for cropping systems. Thus, to analyze L3 we compared IBGE (Brazilian Institute of Geography and Statistics) census data for each municipality in the basin with our maps.

3.3. LULC change

Rates of LULC change were calculated based on the continuous rate of change proposed by Puyravaud (2003):

$$LCLUc\ (\%) = \frac{\ln\left(A_2/A_1\right)}{t_2 - t_1}$$

where A indicates the total area occupied by a certain class in time t. The subscripts 1 and 2 represent the earlier and the subsequent year in an analyzed period. LULCc is the rate of change per year expressed in percentage. We analyzed LULC change trajectories in order to address proximate (direct) causes of change. We built transition matrices produced by a pixel-by-pixel identification of the LULC class in an earlier and the subsequent year time. The number of pixels is transformed in area by multiplying the former by the pixel resolution. We explore underlying causes of LULC change in the UXRB by comparing agricultural expansion to market prices of agricultural products and currency exchange rate (the value ratio between Brazilian Real (R$) and America Dollar (US$)) using the Spearman correlation index. The agricultural products incorporated in the analysis were chosen due their representativeness in the area: (1) cattle herd and beef price, (2) soybean production output and price, (3) maize production output and price. Two sets of prices were used, (1) commodity real prices (corrected by inflation) published by the World Bank (http://www.worldbank.org), and (2) prices received by farmers corrected by inflation (IPCA index for February 2018) and published by the Institute of Applied Economic Research (http://www.ipea.gov.br). Agriculture production was acquired from the Brazilian Institute of Geography and Statistics (https://sidra.ibge.gov.br). All calculations were conducted in *R* (R Development Core Team, 2011).

4. Results

4.1. Classification approach

We created a classification scheme based on simple classification routines, remotely sensed information available at no cost, and algorithms that can be implemented in any common and/or free software that offers the possibility of spatial analyses (E.g.: R, GRASS, among others). For this approach, we created a set of rules, classified image mosaics and product accuracy checks based on ground reference points. We expanded the classification scheme to the years 2010, 2005, 2000, 1995, 1990, and 1985 to identify the main changes in LULC. All derived maps are presented in Supplementary material 5. To apply this classification approach in the UXRB, we processed 12 Landsat (1 mosaic) and ~182 MODIS images (~45 mosaics) for each year. Some critical years required more images to double check spectral quality and to replace cloud covered scenes.

4.2. Accuracy and class separability

We built a three-level hierarchical model (Fig. 2) for image classification with increasing output detail at each level which, thus, presents increasing input and computational demand, and an overall decrease in accuracy (Table 2, Supplementary material 4 for full error matrices). The comparison of our validation database with the produced maps shows that the fraction of correctly classified sample points (overall agreement), considering the proportion of each LULC class in the UXRB, ranged from 84% to 93%. When decomposing the disagreement, all levels presented higher disagreement in quantity than in allocation (Table 2).

All classes presented satisfactory agreement when considering their extension in the area - equal to or lower than 7%, independent of the level of classification. The highest disagreement percentages were observed in cultivated areas in L1 (6%), forest and pasturelands in L2 (7% each), and in forest and pasturelands in L3 (7% each). Forest class error was composed mostly of commission error and quantity disagreement, indicating they were overestimated. Pasturelands in both L1 and L2 presented a balanced error between omission and commission, as well as for quantity and allocation disagreement, indicating both overestimation and spatial dislocation.

When not considering class extension and calculating accuracy directly from observed matrix values, few classes present lower accuracy than expected. In L2, secondary complex and bare land present commission errors of 52% and 54%, respectively. In L3, woody Cerrado (39%), shrub-grassland Cerrado (76%), secondary complex (59%), degraded pasturelands (57%), and bare soil (44%) presented higher omission and commission error percentages. Still, L1 presented great accuracy for all classes. This result was expected, since L1 class separability based on Landsat bands is highly reliable (See Supplementary Material 5 – Fig. 1 for spectral profile). L2 classification is dependent on Level 1, and requires the use of the spectral indexes DGEI and NDVI to separate croplands from pasturelands, and pasturelands from bare soil (Fig. 3). Natural covers could still be separated from Landsat band data (Fig. 2 in Supplementary material 5). L3 classification was dependent on previous levels and thus represents the most complex model, requiring multiple indices to separate classes. Classes with higher separability, such as dense forest, and double cropping systems, presented the highest accuracy (Fig. 4). Degraded pasturelands were mostly confused with pastureland, indicating that we set a conservative rule when separating those classes.

When we compare our mapping results to those obtained by other institutions using different mapping schemas of remote sensing classification (Table 3), we also achieved high values of overall agreement, indicating a high correspondence among them. However, it is important to highlight that LULC validation analyses based on databases created for other purposes should not be considered as accurate as the analysis produced from our validation dataset. Data from other sources contain their own errors, inherent in their production, in addition to errors which may arise from legend adaptation. Furthermore, IBGE data for planted cropland area also supports our methodology, as we found 99% correspondence between this survey and our classified maps through

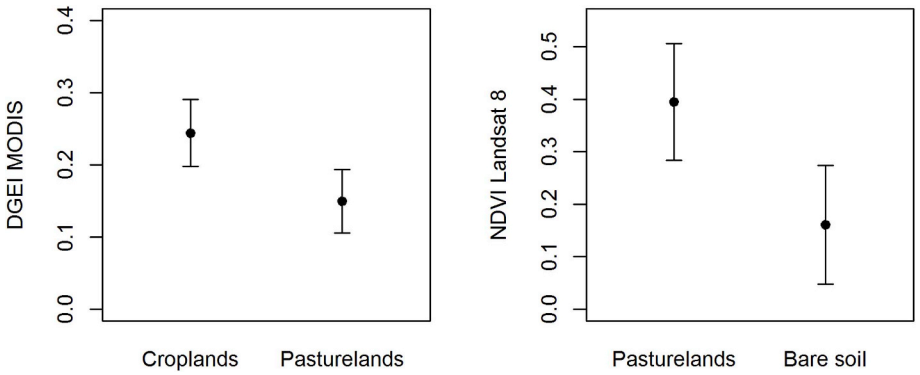

Fig. 3. Separability between (a) croplands and pasturelands derived from the differential greenness enhancement index (DGEI) calculated from MODIS; and (b) pasturelands and bare soil derived from NDVI calculated from Landsat. Values were extracted based in ground reference points collected to assess classification accuracy.

time (see Fig. 5 and the Supplementary material 4 for graphic by municipality).

4.3. LULC change in the UXRB

The period with the highest natural vegetation loss rate in the UXRB was observed to be between 2000 and 2005 (- 5%. Year^{-1}), while the average rate was about – 2%. Year^{-1}. According to L2 mapping, before 1995, most land use change occurred in the savanna formations (9500 km^2 of ~17,000 km^2), and resulted primarily from pasture expansion (Fig. 6; See Supplementary material 7 for transition and area tables). From 1995 to 2010, expansion grew mainly over forested areas, while from 2010 to 2015, savanna formations have again been the main target of agricultural expansion. The observed rates of deforestation between 1995 and 2005 can be spatially divided into two main expansion axes. Until 2000, land use change was most intense at the east and southeast bounds of the UXRB, with large areas of tropical forest converted into pasturelands (~30,000 km^2). From 2000 to 2005, when the highest rates of deforestation were observed, forest clearing occurred mainly in the western portion of the basin and represented both crop and pastureland expansion.

While the highest rates of pasture and crop expansion occurred, respectively, between 1990-1995 and 1995–2005, rates dropped to among the lowest between 2005 and 2010. This last period was also marked by the largest spread of intensification according to L3 mappings - 15% of pasturelands became croplands, and 25% of single crop systems became double cropping systems (Fig. 7; See Supplementary material 7 for transition and area tables). Additionally, pastureland decreased in size during this period, as did the rate of improvement of degraded pasturelands. In this period, cropland expansion rate slightly

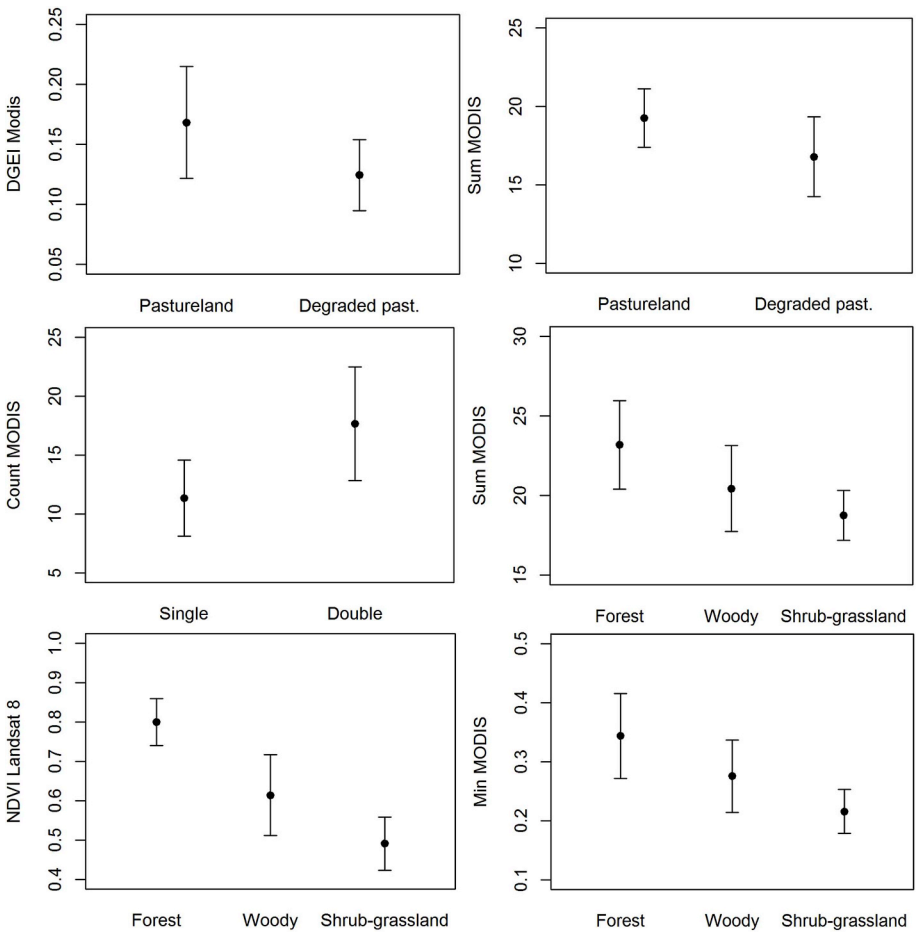

Fig. 4. Separability between classes proposed for classification at level 3. Pasturelands and degraded pasturelands are compared derived from the differential greenness enhancement index – DGEI (a) and the sum of EVI values through a year – SUM (b). Single and double cropping systems are compared based on how many days along the year an EVI > 0.5 is present – COUNT(c). Forest, woody and shrub-grassland, all different savanna physiognomies, are compared based on SUM (d), NDVI values (e), and the minimal EVI value through a year (f). Values were extracted based on ground reference points collected to assess classification accuracy.

Table 3
Overall agreement, quantity disagreement, and allocation disagreement calculated when compared to different databases collected in different years. The information corresponds to the LULC classification of the UXRB (Brazil) in 3 levels of information. Databases were developed by *Instituto de Pesquisa Ambiental da Amazônia* (IPAM) and *Instituto Socioambiental* (ISA).

IPAM database (2017)			
	L1	L2	L3
Agreement (%)	79.96	75.38	64.49
Quantity disagreement (%)	13.41	20.41	15.18
Allocation disagreement (%)	6.63	4.21	20.33
ISA database (2010)			
	L1	L2	L3
Agreement (%)	88.97	90.54	–
Quantity disagreement (%)	9.43	5.69	–
Allocation disagreement (%)	1.60	3.77	–
ISA database (2015)			
	L1	L2	L3
Agreement (%)	95.85	94.22	–
Quantity disagreement (%)	2.07	2.99	–
Allocation disagreement (%)	2.08	2.78	–

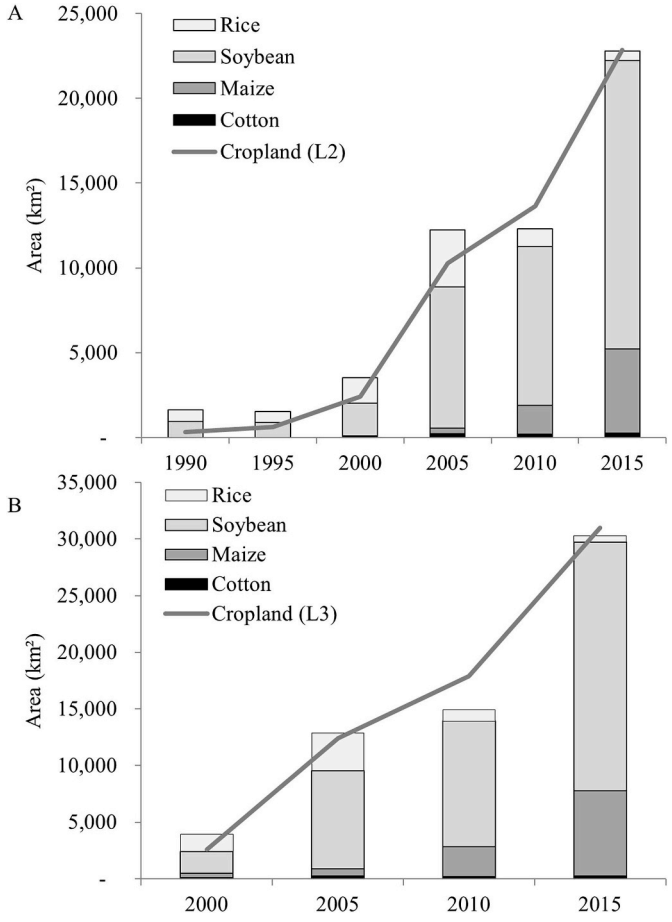

Fig. 5. Correlation between the LULC maps produced for UXRB for croplands and the census data made available by IBGE for the top four crops (rice, soybean, maize and cotton). (A) Lines show the evolution of cropland according to L2 classification while bars show planted area data according to IBGE for rice, soybean discounting secondary maize area (double cropping), main crop maize, and cotton. (B) Lines show the evolution of cropland (accounting twice for double cropping areas) according to L3 classification while bars show planted area data according to IBGE for rice, soybean, maize, and cotton. Data is available by municipality in Supplementary material 4 – Fig. 2.

decreased. With the exception of double crop system, cropland expansion rates increased again between 2010 and 2015. From 2010 to 2015, we observed the largest conversion of pastureland into single or double cropping agricultural systems (~9000 km^2), while conversion of native vegetation, mainly Cerrado formations, increased again (~6500 km^2 of cerrado and ~2500 km^2 of forest were converted into crop systems and pastureland). Additionally, degraded pastureland area also increased during this period.

As expected, the expansion of harvested area and cattle herd is positively correlated with prices and the exchange rate between American Dollar and Brazilian Real (Table 4). For example, the observed peak in the rate of change for cropland (2000–2005) overlaps with the highest prices received by producers in the analyzed period (see Supplementary Material 7 for figures). Still, the exchange rate presented a significantly higher correlation to the expansion of agriculture production than commodity prices.

5. Discussion

5.1. LULC classification and legend

The proposed classification scheme and legend produced spatially explicit information on LULC for the UXRB with more accuracy than we would expect if using global or national products. Besides presenting an overall accuracy between 69 and 78%, global land cover products achieve poor agreement among themselves in tropical ecotones and diverse landscapes (Herold et al., 2008). By design, regional LULC maps derived from satellite images generally present higher levels of accuracy than global mapping schemas because of their intrinsic variability. Our corresponding product (L2) produced an overall accuracy of 86% for the UXRB. Recently produced regional LULC datasets that encompass the UXRB at least partially, also offer information on the study area. The TerraClass Cerrado has an ~80% overall accuracy (Scaramuzza et al., 2017), while TerraClass Amazonia's accuracy is ~77% (Almeida et al., 2016). Still, these mapping schemes present a simpler legend assessment when compared to our hierarchical approach proposed here at L3, and a poorer performance than both L2 (86% accuracy) and L3 (83% accuracy). Additionally, both datasets together do not provide information for the whole studied area, since no mapping data exists for a large portion of the ecotone zone between the Amazon and Cerrado biomes located inside the TerraClass Amazonia study area.

Also, our accuracy analyses showed similar or higher indexes than others studies applied to similar regions and scale. Sawakuchi et al., (2013) applied classification schemes at the Middle Araguaia River Basin, reaching an overall accuracy of 85%, based on 287 ground reference points and delivering a legend which fits in-between our L1 and L2 classifications. Walker et al. (2010) also proposed a hierarchical and multi-level classification approach and applied it to the UXRB. Using a random forest algorithm, and PALSAR- and Landsat-based data, they obtained an overall accuracy from 58% (15 classes) to 92% (2 classes), depending on the classification level. However, all three studies, including ours, achieved poorer results for separating (i) Cerrado land covers, and (ii) pasturelands and degraded pasturelands. Degraded pastureland is an especially important land cover type due to its link to food security and conservation. Even though some studies show an intensification pattern related to improvement in the Brazilian pasturelands since 2005 (Parente and Ferreira, 2018), we believe that degraded pasture is underestimated in our study. The thresholds we implemented linked to the hysteresis principle were likely too conservative.

Few studies have been carried out to improve separability among Cerrado vegetation physiognomies based on remote sensing products. Vegetation indices (VIs) derived from MODIS and calculated indices based on VIs have shown a capacity to separate major physiognomies (Ratana et al., 2005); however, Landsat-simulated VIs presented a

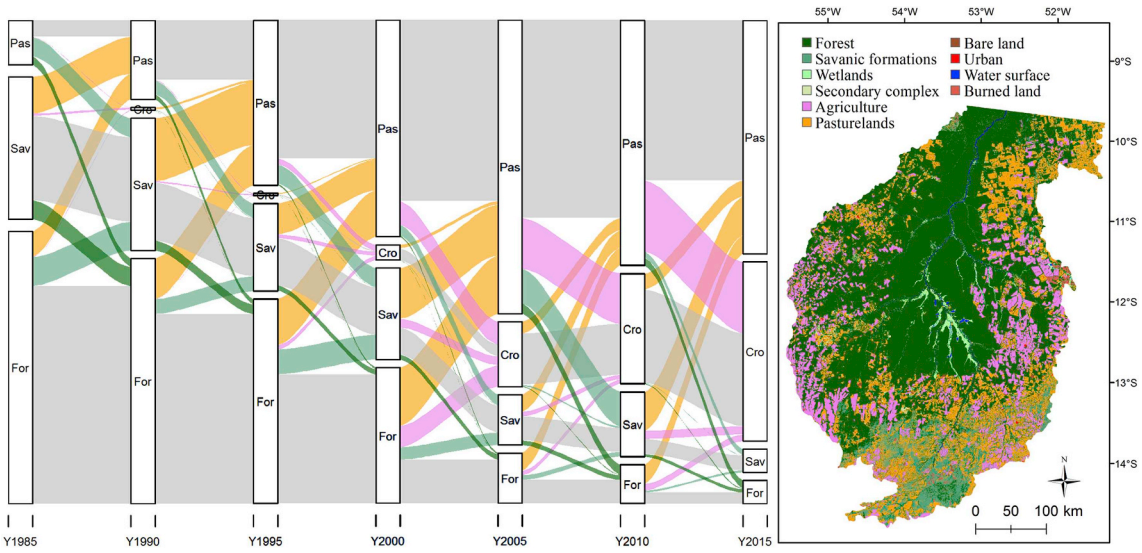

Fig. 6. Land use and land cover transition for all pixels that have changed through time and in non-protected areas in the Upper Xingu River Basin from 1985 to 2015, according to level 2 of classification. The vertical boxes represent the proportion of the Upper Xingu River Basin which each land use occupies in a certain year. The flux lines represent the land use and land cover change. The width of each line represents the proportional amount of land being converted into another use, while each color represents the use it was turned into. The color scheme follows the legend of the map which shows the land use and land cover distribution in 2015.

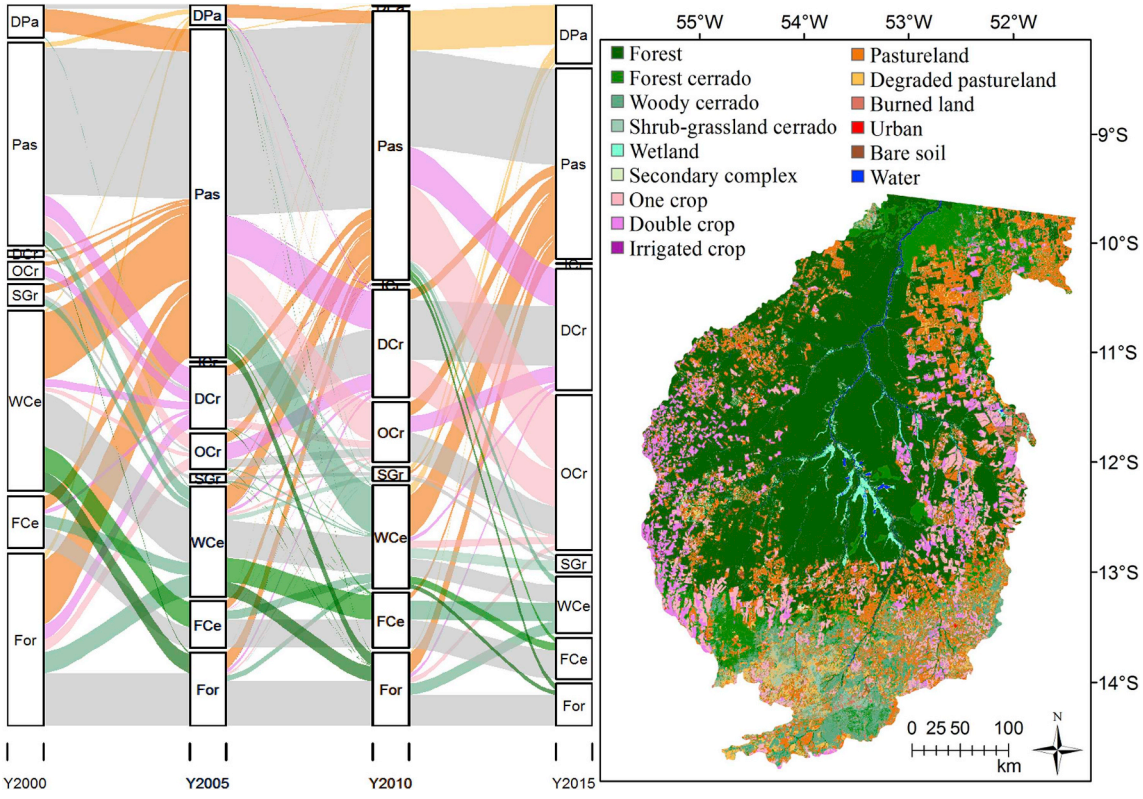

Fig. 7. Land use and land cover transition for all pixels that have changed through time and in non-protected areas in the Upper Xingu River Basin from 2000 to 2015, according to level 3 of classification. The vertical boxes represent the proportion of the Upper Xingu River Basin which each land use occupies in a certain year. The flux lines represent the land use and land cover change. The width of each line represents the proportional amount of land being converted into another use, while each color represents the use it was turned into. The color scheme follows the legend of the map which shows the land use and land cover distribution in 2015.

better discrimination capability when compared to these methods (Ferreira et al., 2003). In our study at the UXRB, even when employing MODIS and Landsat EVI data together, the overall accuracy for Cerrado physiognomy separability was 61% (L3) when not weighting the full class extension, and even lower values were found for shrub-grassland formations. Since shrub-grassland encompasses only 1% of the landscape, and due to the few samples obtained in field surveys, these results are possibly associated with a poor set of rules in the classification process leading to low accuracy values. Still, the results suggest that further attention should be given to studying the temporal pattern of spectral responses in different Cerrado formations. Toniol et al. (2017) evaluated four classifiers for discriminating Cerrado physiognomies in the rainy and dry seasons, and obtained overall accuracies from 26% to 84%, depending on the classifier, season, and metrics used.

Table 4
Spearman correlation and the corresponding significance at 95% (*) and 99% (**) confidence level between main agriculture products (cattle herd, harvested area of soybean and maize accounting for double crop systems), commodities prices (World Bank), price received by the producers (IPEA), and exchange rate between American Dollar and Brazilian Real (Central Bank of Brazil). One year lagged tests presented very similar results.

	Cattle herd	Soybeans area	Maize area
Commodity price (US$)	–	0.56*	0.56**
Price received by producers (R$)	0.51*	0.62**	–
Exchange rate (US$:R$)	0.77**	0.84**	0.81**

MODIS derived VI temporal profiles have also been applied to classify managed land, specifically to extract croplands and to derive crop-specific classes (Brown et al., 2007, 2013). Most of these studies have been based on modelling annual VI records instead of single indices (Rizzi et al., 2009). Aside from the simplicity of using indices such as DGEI or COUNT, one advantage of such method compared to other approaches is that there is no need to define a time period. In other words, these indices can be applied to other regions that do not necessarily present the same agricultural calendar, allowing their use at regional and global mapping scales. In DGEI calculation, the period of time used can be much broader than the sowing-growth window (as applied here), avoiding seasonal changes.

We achieved a more realistic and representative approach using a segmentation-based approach to turn managed areas into objects, and turning those objects into analysis units (Blaschke, 2010). Through this approach we, avoided problems such as pixel heterogeneity, mixed pixels, and spectral similarity due to crop or pastureland spatial variability (Peña-Barragán et al., 2011; Yu et al., 2016). Additionally, while classification approaches often present a larger allocation disagreement than quantity disagreement, our results shows the opposite (E.g.: Pontius et al. (2011)). It suggests that the combined pixel and object approach represents the land configuration better than automatic per-pixel classification methods. Still, the techniques used in this research may not favor mapping of small producers and permanent crops. Such analysis is out of the scope of this research, but it is encouraged for future studies. Indices other than the ones used in this study, such as a clumping index, were not reported to significantly improve separability in neotropical savannas and are highly correlated with VI (Hill et al., 2011). We encourage the application of object-oriented approaches and indices derived from temporal composition in other classification methods, such as machine learning.

The proposed classification approach allowed us to analyze a more complex and realistic scenario of LULC change in the UXRB, and thus address issues related to expansion and intensification, biome specific dynamic changes, and cropland and pastureland roles in native vegetation loss. The high accuracy values attributed to L1 and the applied legend make this level of classification suitable for studies on law and policy enforcement (Goetz et al., 2015). L2 addresses general differences in land use and land cover, offering a reliable product to model ecosystem dynamics such as regional hydrological balance (Dwarakish and Ganasri, 2015). The third level of classification offers further information on regional LULC by addressing vegetative productivity. It allows users to address issues related to habitat suitability and priority areas for conservation by separating native vegetation physiognomies. Such separability issues are even more important and challenging for the Cerrado biome. Although it is recognized as the richest savanna in the world and a hotspot for conservation (Klink and Machado, 2005; Myers et al., 2000), it is still not a major focus of policies and research, nationally or internationally (Nolte et al., 2017). This pattern is related to the lack of monitoring techniques and knowledge of ecological dynamics taking place in the biome. Our proposed methodology offers insights into monitoring techniques and encourages further research. The third level of classification also makes it possible to address food production, land management, and the relationship between productive systems and socioeconomic dynamics. The intensified use of agricultural lands is a key discussion topic related to both land sparing for conservation (Ewers et al., 2009) and socioeconomic development (Martinelli et al., 2017). Still, a clear drawback of the hierarchical approach used in this study is the nested dependency between levels of classification since L3 is dependent on L2, and L2 is dependent on L1. Possible ways of mitigating this problem include assigning a smaller weight to classified maps when using them as source of information in another level of classification, or even avoiding altogether the use of one classified map in the modelling of another level of classification.

5.2. LULC changes in the UXRB

Until 2000, LULC change in UXRB was primarily driven by pastureland expansion following patterns observed in Amazon and Cerrado biomes (Ferreira et al., 2012; INPE, 2018). In 1990s and 2000s, the region transitioned from a pioneer landscape to a consolidated frontier, in which agro-production moved from a labor-intensive system to one based on financial capital and integration into market. The consolidation of cattle production in the 90s occurred in all states on the southern frontier of the Amazon (Margulis, 2004). From 2000 to 2015, land use transitions in the UXRB indicated an intensification process, which was manifested through an increase in cultivated area over pastureland, accompanied by a large reduction in deforestation. Intensification processes are a result of environmental regulations, technological changes, economic disincentives for deforestation, and/or market regulations (Gasparri and de Waroux, 2015). By the end of the study period, the UXRB became a frontier which supplies both international and regional markets.

Reductions in deforestation, combined with crop expansion, have been described for the Brazilian biomes in the last decades (Dias et al., 2016; Macedo et al., 2012). Brando et al. (2013) shed light on how the actions of different stakeholders (e.g.: government – zero deforestation act, private sector – soy moratorium, and non-profit organizations through multiple campaigns) helped to reduce deforestation in the UXRB during the 2000s. With available technology, producers were able to increase yields in order to increase profits. However, our analysis shows that intensification is biome-dependent. We observed an increase in agricultural intensification mainly in the Amazon region of the UXRB, between 2000 and 2005, and 2010–2015. This temporal pattern is correlated with peaks in the exchange rate, and secondarily with commodity prices. Expansion is still the dominant LULC change process in the Cerrado portion of the UXRB, as it is for the Cerrado biome as whole (Lapola et al., 2013). This expansion can be confirmed as we observe a reduction of 20% in savanic formation from 2010 to 2015, a value 10 times higher than the one found for the amazon forest over the same period. The conversion from woody Cerrado to pastureland accounts for the majority of these changes. This process is correlated with an increase in beef prices. But the low number of conservation areas, as well as the lack of market regulation and effective deforestation control programs, are the main differences between protection schemes in the Cerrado and the Amazon biomes (Gibbs et al., 2015; Sparovek et al., 2010). According to intensification theories, without those mechanisms of incentive or control, intensification will not be encouraged (Meyfroidt et al., 2018).

Cash crops primarily replace pasturelands in the UXRB, followed by cerrado formations and Amazonian forest - mainly between 2000-2005 and 2010–2015. Those results are partially in accordance with Macedo (Macedo et al., 2012), which underestimated native vegetation loss at the cerrado region in the UXRB due to cash crop expansion. Rather than intensification and regulation effects, the lower conversion of native vegetation into croplands observed between 2005 and 2010 is a result of market and currency exchange effects pushing soybean prices down (Richards et al., 2012). The increase in native vegetation loss again from 2010 to 2015 supports this idea, together with the hypothesis that

intensification does not necessarily lead to decreases in the expansion of agricultural frontiers (Barretto et al., 2013; Rudel et al., 2009). Although our goal was not to analyze indirect frontier development through land use change, the displacement of cattle production by cash crops has been observed in the UXRB and elsewhere (Barona et al., 2010; Fehlenberg et al., 2017; Macedo et al., 2012). Aditionally, increased land market values in areas of soybean expansion have been shown to drive migration-based development (Richards, 2015). The increase in deforestation in the Cerrado compared to the Amazon portion of the basin can be considered evidence of a rebound effect. Theories concerning this effect state that technology, policies, and market-drive the intensification of land use as observed in the Amazon portion of the UXRB (Meyfroidt et al., 2018). Land sparing is observed in a region when land use is restricted by regulations and, as a consequence, production price per area increases due to a required disaggregation of production area. Conversely, expansion is observed elsewhere as a rebound effect when land with limited regulations is available – such as in the Cerrado biome (Soares-Filho et al., 2014); and the production is focused on products for which the prices are elastic based on demand - such as soybean (Heien and Pick, 1991; Meyfroidt et al., 2018).

6. Conclusions

Tropical ecotone zones and agricultural frontiers, such as the UXRB, are important for Neotropical biosociodiversity and for agricultural production. However, their inherent complexity poses challenges for LULC change analyses and LULC planning. The combination of multiple classification techniques, as well as the combination of remote sensing and GIS-based information which assesses temporal variability, have been reported as superior approaches compared to traditional techniques. Our proposed classification scheme uses an unsupervised classification approach to initially group pixels into few classes. These classes are then reclassified through decision trees by the integration of multi-sensor and GIS data into an object and pixel context. The multi-data, -temporal and -spatial scale characteristics of the analyses were crucial to maintaining high spatial resolution and the high amount of information throughout the hierarchal classification. Furthermore, the approaches applied here can give insights into continental and global mapping processes such as the use of metrics based on flexible time series with no need to define fixed starting and ending dates. Still, to transfer the methodology to other study areas, thresholds and information should be adapted.

Because of their ability to discriminate between different LULC in complex environments, the LULC products created in this research enabled us to differentiate between different processes that drive agricultural production increases in the UXRB. Beside our observation that the increase in agricultural production in the UXRB being generally correlated with commodity prices and monetary exchange rates, we were also able to map different processes affecting production (expansion, intensification, and degradation). For instance, the area in the basin which overlaps with the Amazon biome experiences intensification, while the Cerrado biome experiences expansion. This result is mainly linked to government and market regulations, which are focused in the Amazon but are lacking in the Cerrado biome.

Funding

This work was supported by the Belmont Forum/funded Xingu project (“Integrating land use planning and water governance in Amazonia: towards improved freshwater security in the agricultural frontier of Mato Grosso”) via São Paulo Research Foundation (FAPESP), grant number 2013/50180-5); Andrea Garcia is recipient of grant 2015/05103-8 and 2017/12787-6 from FAPESP; Rodnei Rizzo is recipient of grant 2013/20377-1 and 2017/12567-6 from FAPESP. Andrea Garcia, Vivian Vilela, and Rodnei Rizzo were also recipients of grants from CAPES, and Maria Victoria Ballester from CNPq. Paul West and James Gerber received support from the Belmont Forum/FACCE-JPI funded DEVIL project (Delivering Food Security from Limited Land) (NE/M021327/1) via NSF award no. 1540195. We also thank Instituto Socioambiental (ISA) and Instituto de Pesquisa Ambiental da Amazônia (IPAM) for making data available, contributing to this manuscript.

Acknowledge:

We thank the Brazilian Ministry of the Environment to make available high-resolution satellite images through the “GEO CATALOGO”.

Appendix A. Supplementary data

Supplementary data to this article can be found online at https://doi.org/10.1016/j.rsase.2019.05.002.

References

Aguirre-Gutiérrez, J., Seijmonsbergen, A.C., Duivenvoorden, J.F., 2012. Optimizing land cover classification accuracy for change detection, a combined pixel-based and object-based approach in a mountainous area in Mexico. Appl. Geogr. 34, 29–37. https://doi.org/10.1016/j.apgeog.2011.10.010.

Almeida, C.A. de, Coutinho, A.C., Esquerdo, J.C.D.M., Adami, M., Venturieri, A., Diniz, C.G., Dessay, N., Durieux, L., Gomes, A.R., 2016. High spatial resolution land use and land cover mapping of the Brazilian Legal Amazon in 2008 using Landsat-5/TM and MODIS data. Acta Amazonica 46, 291–302. https://doi.org/10.1590/1809-4392201505504.

Arvor, D., Meirelles, M., Dubreuil, V., Bégué, A., Shimabukuro, Y.E., 2012. Analyzing the agricultural transition in Mato Grosso, Brazil, using satellite-derived indices. Appl. Geogr. 32, 702–713. https://doi.org/10.1016/j.apgeog.2011.08.007.

Azzari, G., Lobell, D.B., 2017. Landsat-based classification in the cloud: An opportunity for a paradigm shift in land cover monitoring. Remote Sens. Environ. https://doi.org/10.1016/j.rse.2017.05.025.

Barona, E., Ramankutty, N., Hyman, G., Coomes, O.T., 2010. The role of pasture and soybean in deforestation of the Brazilian Amazon. Environ. Res. Lett. 5, 024002. https://doi.org/10.1088/1748-9326/5/2/024002.

Barretto, A.G.O.P., Berndes, G., Sparovek, G., Wirsenius, S., 2013. Agricultural intensification in Brazil and its effects on land-use patterns: An analysis of the 1975-2006 period. Glob. Chang. Biol. 19, 1804–1815. https://doi.org/10.1111/gcb.12174.

Bartholomé, E., Belward, A.S., 2005. GLC2000: A new approach to global land cover mapping from Earth observation data. Int. J. Remote Sens. 26, 1959–1977. https://doi.org/10.1080/01431160412331291297.

Blaschke, T., 2010. Object based image analysis for remote sensing. ISPRS J. Photogrammetry Remote Sens. https://doi.org/10.1016/j.isprsjprs.2009.06.004.

Bondeau, A., Smith, P.C., Zaehle, S., Schaphoff, S., Lucht, W., Cramer, W., Gerten, D., Lotze-campen, H., Müller, C., Reichstein, M., Smith, B., 2007. Modelling the role of agriculture for the 20th century global terrestrial carbon balance. Glob. Chang. Biol. 13, 679–706. https://doi.org/10.1111/j.1365-2486.2006.01305.x.

Brando, P.M., Coe, M.T., DeFries, R., Azevedo, A.A., 2013. Ecology, economy and management of an agroindustrial frontier landscape in the southeast Amazon. Philos. Trans. R. Soc. Lond. B Biol. Sci. 368, 9. https://doi.org/10.1098/rstb.2012.0152.

Brasil/MMA, 2018. O Bioma Cerrado. Brazil/MMA, 2018. (Amazônia).

Brown, J., Jepson, W., Kastens, J., Wardlow, B., Lomas, J., Price, K., 2007. Multitemporal, moderate-spatial-resolution remote sensing of modern agricultural production and land modification in the Brazilian amazon. GIScience Remote Sens. 44, 117–148. https://doi.org/10.2747/1548-1603.44.2.117.

Brown, J.C., Kastens, J.H., Coutinho, A.C., Victoria, D. de C., Bishop, C.R., 2013. Classifying multiyear agricultural land use data from Mato Grosso using time-series MODIS vegetation index data. Remote Sens. Environ. 130, 39–50. https://doi.org/10.1016/j.rse.2012.11.009.

Chen, Y., Zhou, Y., Ge, Y., An, R., Chen, Y., 2018. Enhancing land cover mapping through integration of pixel-based and object-based classifications from remotely sensed imagery. Rem. Sens. 10, 77. https://doi.org/10.3390/rs10010077.

Coppin, P., Jonckheere, I., Nackaerts, K., Muys, B., Lambin, E., 2004. Digital change detection methods in ecosystem monitoring: A review. Int. J. Remote Sens. 25, 1565–1596. https://doi.org/10.1080/0143116031000101675.

de Chazal, J., Rounsevell, M.D.A., 2009. Land-use and climate change within assessments of biodiversity change: A review. Glob. Environ. Chang. 19, 306–315. https://doi.org/10.1016/j.gloenvcha.2008.09.007.

Di Gregorio, A., 2016. Land Cover Classification System. FAO, Rome.

Di Gregorio, A., Jansen, L.J.M., 2000. Land cover classification system (LCCS): Classification concepts and user manual. Fao 53, 179. https://doi.org/10.1017/CBO9781107415324.004.

Dias-Filho, M.B., 2001. Degradação de Pastagens: Processos, causas e estratégias, 4º. ed, Degradação de Pastagens: Processos, causas e estratégias. MBDF. (Belém).

Dias, L.C.P., Pimenta, F.M., Santos, A.B., Costa, M.H., Ladle, R.J., 2016. Patterns of land use, extensification, and intensification of Brazilian agriculture. Glob. Chang. Biol. https://doi.org/10.1111/gcb.13314.

Döll, P., Kaspar, F., Lehner, B., 2003. A global hydrological model for deriving water

availability indicators: Model tuning and validation. J. Hydrol. 270, 105–134. https://doi.org/10.1016/S0022-1694(02)00283-4.
Don, A., Schumacher, J., Freibauer, A., 2011. Impact of tropical land-use change on soil organic carbon stocks - a meta-analysis. Glob. Chang. Biol. 17, 1658–1670. https://doi.org/10.1111/j.1365-2486.2010.02336.x.
Dwarakish, G.S., Ganasri, B.P., 2015. Impact of land use change on hydrological systems: A review of current modeling approaches. Cogent Geosci. 1. https://doi.org/10.1080/23312041.2015.1115691.
ERDAS, 2014. ERDAS Imagine.
ERDAS, 2014. Knowledge Engineer.
Endo, A., Tsurita, I., Burnett, K., Orencio, P.M., 2015. A review of the current state of research on the water, energy, and food nexus. J. Hydrol. Reg. Stud. https://doi.org/10.1016/j.ejrh.2015.11.010.
Ewers, R.M., Scharlemann, J.P.W., Balmford, A., Green, R.E., 2009. Do increases in agricultural yield spare land for nature? Glob. Chang. Biol. 15, 1716–1726. https://doi.org/10.1111/j.1365-2486.2009.01849.x.
FAO, 2011. The State of the World's Land and Water Resources for Food and Agriculture (SOLAW) - Managing Systems at Risk. Food and Agriculture Organization of the United Nations, Rome, and Earthscan, London.
FAO, 1993. Guidelines for Land-Use Planning FAO Develo, vol. 96. pp. 96.
FAOSTAT, 2016. Country Indicators.
Fehlenberg, V., Baumann, M., Gasparri, N.I., Piquer-Rodriguez, M., Gavier-Pizarro, G., Kuemmerle, T., 2017. The role of soybean production as an underlying driver of deforestation in the South American Chaco. Glob. Environ. Chang. 45, 24–34. https://doi.org/10.1016/j.gloenvcha.2017.05.001.
Ferreira, L.G., Sano, E.E., Fernandez, L.E., Araújo, F.M., 2013. Biophysical characteristics and fire occurrence of cultivated pastures in the Brazilian savanna observed by moderate resolution satellite data. Int. J. Remote Sens. 34, 154–167. https://doi.org/10.1080/01431161.2012.712223.
Ferreira, L.G., Yoshioka, H., Huete, A., Sano, E.E., 2003. Seasonal landscape and spectral vegetation index dynamics in the Brazilian Cerrado: An analysis within the Large-Scale Biosphere-Atmosphere Experiment in Amazônia (LBA). Remote Sens. Environ. 87, 534–550. https://doi.org/10.1016/j.rse.2002.09.003.
Ferreira Jr., M.E., L.G.F., Miziara, F., Soares, B.S., Ferreira, L.G., Miziara, F., Soares-Filho, B.S., 2012. Modeling landscape dynamics in the central Brazilian savanna biome: Future scenarios and perspectives for conservation. J. Land Use Sci. 4248, 1–19. https://doi.org/10.1080/1747423X.2012.675363.
Foley, J.A., Defries, R., Asner, G.P., Barford, C., Bonan, G., Carpenter, S.R., Chapin, F.S., Coe, M.T., Daily, G.C., Gibbs, H.K., Helkowski, J.H., Holloway, T., Howard, E.A., Kucharik, C.J., Monfreda, C., Patz, J. a, Prentice, I.C., Ramankutty, N., Snyder, P.K., 2005. Global consequences of land use. Science 309, 570–574. https://doi.org/10.1126/science.1111772.
Friedl, M.A., Sulla-Menashe, D., Tan, B., Schneider, A., Ramankutty, N., Sibley, A., Huang, X., 2010. MODIS Collection 5 global land cover: Algorithm refinements and characterization of new datasets. Remote Sens. Environ. 114, 168–182. https://doi.org/10.1016/j.rse.2009.08.016.
Gasparri, N.I., de Waroux, Y. le P., 2015. The coupling of South American soybean and cattle production frontiers: New challenges for conservation policy and land change science. Conserv. Lett. 8, 290–298. https://doi.org/10.1111/conl.12121.
Ge, J., Qi, J., Lofgren, B.M., Moore, N., Torbick, N., Olson, J.M., 2007. Impacts of land use/cover classification accuracy on regional climate simulations. J. Geophys. Res. 112, D05107. https://doi.org/10.1029/2006JD007404.
Gibbs, H.K., Rausch, L., Munger, J., Schelly, I., Morton, D.C., Noojipady, P., Soares-Filho, B., Barreto, P., Micol, L., Walker, N.F., 2015. Brazil's soy moratorium. Science 347, 377–378. https://doi.org/10.1126/science.aaa0181.
Giri, C., Zhu, Z., Reed, B., 2005. A comparative analysis of the Global Land Cover 2000 and MODIS land cover data sets. Remote Sens. Environ. 94, 123–132. https://doi.org/10.1016/j.rse.2004.09.005.
Goetz, S.J., Hansen, M., Houghton, R.A., Walker, W., Laporte, N., Busch, J., 2015. Measurement and monitoring needs, capabilities and potential for addressing reduced emissions from deforestation and forest degradation under REDD+. Environ. Res. Lett. https://doi.org/10.1088/1748-9326/10/12/123001.
Gómez, C., White, J.C., Wulder, M.A., 2016. Optical remotely sensed time series data for land cover classification: A review. ISPRS J. Photogrammetry Remote Sens. https://doi.org/10.1016/j.isprsjprs.2016.03.008.
Hansen, M.C., Loveland, T.R., 2012. A review of large area monitoring of land cover change using Landsat data. Remote Sens. Environ. 122, 66–74. https://doi.org/10.1016/j.rse.2011.08.024.
Heien, D., Pick, D., 1991. The Structure of International Demand for Soybean Products. South. J. Agric. Econ. 23, 137–146. https://doi.org/10.1017/S008130520001791X.
Herold, M., Mayaux, P., Woodcock, C.E., Baccini, A., Schmullius, C., 2008. Some challenges in global land cover mapping: An assessment of agreement and accuracy in existing 1 km datasets. Remote Sens. Environ. 112, 2538–2556. https://doi.org/10.1016/j.rse.2007.11.013.
Hill, M.J., Román, M.O., Schaaf, C.B., Hutley, L., Brannstrom, C., Etter, A., Hanan, N.P., 2011. Characterizing vegetation cover in global savannas with an annual foliage clumping index derived from the MODIS BRDF product. Remote Sens. Environ. 115, 2008–2024. https://doi.org/10.1016/j.rse.2011.04.003.
Hussain, M., Chen, D., Cheng, A., Wei, H., Stanley, D., 2013. Change detection from remotely sensed images: From pixel-based to object-based approaches. ISPRS J. Photogrammetry Remote Sens. 80, 91–106. https://doi.org/10.1016/j.isprsjprs.2013.03.006.
IBGE, 2016. Sistema IBGE de Recuperação Automática (SIDRA): banco de dados sobre indicadores, população, economia e geociências.
IBGE, 2004. Mapas de Cobertura Vegetal dos Biomas Brasileiros.
INPE - Instituto Nacional de Pesquisas Espaciais, 2018. Monitoramento da Floresta Amazônica Brasileira por Satélite. São José dos Campos.
Ivanauskas, N.M., Monteiro, R., Rodrigues, R.R., 2008. Classificação fitogeográfica das florestas do Alto Rio Xingu. Acta Amazonica 38, 387–402. https://doi.org/10.1590/S0044-59672008000300003.
Klink, C. a., Machado, R.B., 2005. Conservation of the Brazilian cerrado. Conserv. Biol. 19, 707–713. https://doi.org/10.1111/j.1523-1739.2005.00702.x.
Lapola, D.M., Martinelli, L.A., Peres, C.A., Ometto, J.P.H.B., Ferreira, M.E., Nobre, C.A., Aguiar, A.P.D., Bustamante, M.M.C., Cardoso, M.F., Costa, M.H., Joly, C.A., Leite, C.C., Moutinho, P., Sampaio, G., Strassburg, B.B.N., Vieira, I.C.G., 2013. Pervasive transition of the Brazilian land-use system. Nat. Clim. Change 4, 27–35. https://doi.org/10.1038/nclimate2056.
Lal, R., 2016. Global food security and nexus thinking. J. Soil Water Conserv. 71, 85A–90A. https://doi.org/10.2489/jswc.71.4.85A.
Lathuillière, M.J., Miranda, E.J., Bulle, C., Couto, E.G., Johnson, M.S., 2017. Land occupation and transformation impacts of soybean production in Southern Amazonia, Brazil. J. Clean. Prod. 149, 680–689. https://doi.org/10.1016/j.jclepro.2017.02.120.
Lebourgeois, V., Dupuy, S., Vintrou, É., Ameline, M., Butler, S., Bégué, A., 2017. A combined random forest and OBIA classification scheme for mapping smallholder agriculture at different nomenclature levels using multisource data (simulated Sentinel-2 time series, VHRS and DEM). Rem. Sens. https://doi.org/10.3390/rs9030259.
Lu, D., Mausel, P., Brondízio, E., Moran, E., 2004. Change detection techniques. Int. J. Remote Sens. 25, 2365–2401. https://doi.org/10.1080/0143116031000139863.
Lu, D., Weng, Q., 2007. A survey of image classification methods and techniques for improving classification performance. Int. J. Remote Sens. https://doi.org/10.1080/01431160600746456.
Macedo, M.N., Coe, M.T., DeFries, R., Uriarte, M., Brando, P.M., Neill, C., Walker, W.S., 2013. Land-use-driven stream warming in southeastern Amazonia. Philos. Trans. R. Soc. B Biol. Sci. 368 20120153–20120153. https://doi.org/10.1098/rstb.2012.0153.
Macedo, M.N., DeFries, R.S., Morton, D.C., Stickler, C.M., Galford, G.L., Shimabukuro, Y.E., 2012. Decoupling of deforestation and soy production in the southern Amazon during the late 2000s. Proc. Natl. Acad. Sci. U. S. A 109, 1341–1346. https://doi.org/10.1073/pnas.1111374109.
Margulis, S., 2004. Causes of Deforestation of the Brazilian Amazon. World Bank Work. Pap. 1–77. https://doi.org/10.1596/0-8213-5691-7.
Martinelli, L., Batistella, M., Silva, R., Moran, E., 2017. Soy expansion and socioeconomic development in municipalities of Brazil. Land 6, 62. https://doi.org/10.3390/land6030062.
Masek, J.G., Vermote, E.F., Saleous, N., Wolfe, R., Hall, F.G., Huemmrich, F., Gao, F., Kutler, J., Lim, T.K., 2006. A Landsat surface reflectance dataset for North America, 1990–2000. Geosci. Remote Sens. Lett. 3, 68–72.
Mattiuzzi, M., Hengl, T., Verbesselt, J., Lobo, A., Klisch, A., Evans, B., Stevens, F., Mosher, S., Maspons, J., Detsch, F., Hufkens, K., 2016. MODIS: MODIS acquisition and processing package.
Maxwell, A.E., Warner, T.A., Fang, F., 2018. Implementation of machine-learning classification in remote sensing: An applied review. Int. J. Remote Sens. https://doi.org/10.1080/01431161.2018.1433343.
Meyfroidt, P., Roy Chowdhury, R., de Bremond, A., Ellis, E.C., Erb, K.H., Filatova, T., Garrett, R.D., Grove, J.M., Heinimann, A., Kuemmerle, T., Kull, C.A., Lambin, E.F., Landon, Y., le Polain de Waroux, Y., Messerli, P., Müller, D., Nielsen, J., Peterson, G.D., Rodriguez García, V., Schlüter, M., Turner, B.L., Verburg, P.H., 2018. Middle-range theories of land system change. Glob. Environ. Chang. 53, 52–67. https://doi.org/10.1016/j.gloenvcha.2018.08.006.
Müller, H., Rufin, P., Griffiths, P., Barros Siqueira, A.J., Hostert, P., 2015. Mining dense Landsat time series for separating cropland and pasture in a heterogeneous Brazilian savanna landscape. Remote Sens. Environ. 156, 490–499. https://doi.org/10.1016/j.rse.2014.10.014.
Myers, N., Mittermeier, R.A., Mittermeier, C.G., da Fonseca, G.A.B., Kent, J., 2000. Biodiversity hotspots for conservation priorities. Nature 403, 853–858. https://doi.org/10.1038/35002501.
Nepstad, D.C., Stickler, C.M., Almeida, O.T., 2006. Globalization of the Amazon soy and beef industries: Opportunities for conservation. Conserv. Biol. https://doi.org/10.1111/j.1523-1739.2006.00510.x.
Nolte, C., le Polain de Waroux, Y., Munger, J., Reis, T.N.P., Lambin, E.F., 2017. Conditions influencing the adoption of effective anti-deforestation policies in South America's commodity frontiers. Glob. Environ. Chang. 43, 1–14. https://doi.org/10.1016/j.gloenvcha.2017.01.001.
Ozturk, I., 2015. Sustainability in the food-energy-water nexus: Evidence from BRICS (Brazil, the Russian Federation, India, China, and South Africa) countries. Energy 93, 999–1010. https://doi.org/10.1016/j.energy.2015.09.104.
Oliveira, P., Marquis, R., ... 2002. The Cerrados of Brazil, The Cerrados. https://doi.org/10.1663/0013-0001 (2003)057[0656:DFABRE]2.0.CO;2.
Parente, L., Ferreira, L., 2018. Assessing the Spatial and Occupation Dynamics of the Brazilian Pasturelands Based on the Automated Classification of MODIS Images from 2000 to 2016. Rem. Sens., vol. 10. https://doi.org/10.3390/rs10040606.
Peña-Barragán, J.M., Ngugi, M.K., Plant, R.E., Six, J., 2011. Object-based crop identification using multiple vegetation indices, textural features and crop phenology. Remote Sens. Environ. 115, 1301–1316. https://doi.org/10.1016/j.rse.2011.01.009.
Pendrill, F., Persson, U.M., 2017. Combining global land cover datasets to quantify agricultural expansion into forests in Latin America: Limitations and challenges. PLoS One. https://doi.org/10.1371/journal.pone.0181202.
Pontius, R.G., Millones, M., Pontius, Robert, Gilmore, J., Millones, M., Pontius, R.G., Millones, M., 2011. Death to Kappa: Birth of quantity disagreement and allocation disagreement for accuracy assessment. Int. J. Remote Sens. 32, 4407–4429. https://doi.org/10.1080/01431161.2011.552923.
Power, A.G., 2010. Ecosystem services and agriculture: Tradeoffs and synergies. Philos.

Trans. R. Soc. B Biol. Sci. 365, 2959–2971. https://doi.org/10.1098/rstb.2010.0143.
Puyravaud, J.P., 2003. Standardizing the calculation of the annual rate of deforestation. For. Ecol. Manage. 177, 593–596. https://doi.org/10.1016/S0378-1127(02)00335-3.
R Development Core Team, R, 2011. R: A Language and Environment for Statistical Computing. R Found. Stat. Comput., R Foundation for Statistical Computing. https://doi.org/10.1007/978-3-540-74686-7.
Ratana, P., Huete, A.R., Ferreira, L., 2005. Analysis of cerrado physiognomies and conversion in the MODIS seasonal-temporal domain. Earth Interact. 9 (2005) 009 < 0001:AOCPAC > 2.0.CO;2. https://doi.org/10.1175/1087-3562.
Richards, P., 2015. What drives indirect land use change? How Brazil's agriculture sector influences frontier deforestation. Ann. Assoc. Am. Geogr. 105, 1026–1040. https://doi.org/10.1080/00045608.2015.1060924.
Richards, P.D., Myers, R.J., Swinton, S.M., Walker, R.T., 2012. Exchange rates, soybean supply response, and deforestation in South America. Glob. Environ. Chang. 22, 454–462. https://doi.org/10.1016/j.gloenvcha.2012.01.004.
Rizzi, R., Risso, J., Epiphanio, R.D.V., Rudorff, B.F.T., Formaggio, A.R., Shimabukuro, Y.E., Fernandes, S.L., 2009. Estimativa da área de soja no Mato Grosso por meio de imagens MODIS. In: Simpósio Brasileiro de Sensoriamento Remoto. INPE, São José dos Campos, pp. 387–394.
Rudel, T.K., Schneider, L., Uriarte, M., Turner, B.L., DeFries, R., Lawrence, D., Geoghegan, J., Hecht, S., Ickowitz, A., Lambin, E.F., Birkenholtz, T., Baptista, S., Grau, R., 2009. Agricultural intensification and changes in cultivated areas, 1970-2005. Proc. Natl. Acad. Sci. Unit. States Am. 106, 20675–20680. https://doi.org/10.1073/pnas.0812540106.
Sawakuchi, H.O., Ballester, M.V., Ferreira, M.E., 2013. The role of physical and political factors on the conservation of native vegetation in the Brazilian forest-savanna ecotone. Open J. For. 03, 49–56. https://doi.org/10.4236/ojf.2013.31008.
Scaramuzza, C.A. de M., Sano, E.E., Adami, M., Bolfe, E.L., Coutinho, A.C., César, J., Mora, D., Eduardo, L., Maurano, P., Narvaes, S., José, F., Oliveira, B., de, Rosa, R., Barbosa, E., Valeriano, D. de M., Victoria, D. de C., Bayma, P., Oliveira, G.H. de, Bayma-Silva, G., 2017. Land-use and land-cover mapping of the Brazilian cerrado based mainly on Landsat-8 satellite images. Rev. Bras. Cartogr. a (2017), Edição Fotogrametia e Sensoriamento Remoto 69, 1041–1051.
Scaramuzza, P., Micijevic, E., Chander, G., 2004. SCL Gap-Filled Products. Phase One Methodology. (USGS-United States Geol. Surv).
Searle, K.R., Gordon, I.J., Stokes, C.J., 2009. Hysteretic responses to grazing in a semiarid rangeland. Rangel. Ecol. Manag. 62, 136–144. https://doi.org/10.2111/08-200.1.
Soares-Filho, B., Rajao, R., Macedo, M., Carneiro, A., Costa, W., Coe, M., Rodrigues, H., Alencar, A., 2014. Cracking Brazil's forest Code. Science 344, 363–364. https://doi.org/10.1126/science.1246663.
Sparovek, G., Berndes, G., Klug, I.L.F., Barretto, A.G.O.P., 2010. Brazilian agriculture and environmental legislation: Status and future challenges. Environ. Sci. Technol. 44, 6046–6053. https://doi.org/10.1021/es1007824.
Tewkesbury, A.P., Comber, A.J., Tate, N.J., Lamb, A., Fisher, P.F., 2015. A critical synthesis of remotely sensed optical image change detection techniques. Remote Sens. Environ. 160, 1–14. https://doi.org/10.1016/j.rse.2015.01.006.
Toniol, A.C., Galvão, L.S., Ponzoni, F.J., Sano, E.E., Amore, D. de J., 2017. Potential of hyperspectral metrics and classifiers for mapping Brazilian savannas in the rainy and dry seasons. Remote Sens. Appl. Soc. Environ. 8, 20–29. https://doi.org/10.1016/j.rsase.2017.07.004.
Turner, B.L., Lambin, E.F., Reenberg, A., 2007. The emergence of land change science for global environmental change and sustainability. Proc. Natl. Acad. Sci. Unit. States Am. 104, 20666–20671. https://doi.org/10.1073/pnas.0704119104.
Velasquez, C., Alves, H.Q., Bernasconi, P., 2010. FIQUE POR DENTRO: a Bacia Do Rio Xingu Em Mato Grosso. nstituto Socioambiental, Instituto Centro de Vida, São Paulo.
Vuolo, F., Mattiuzzi, M., Klisch, A., Atzberger, C., 2012. Data service platform for MODIS Vegetation Indices time series processing at BOKU Vienna: Current status and future perspectives. In: Michel, U., Civco, D.L., Ehlers, M., Schulz, K., Nikolakopoulos, K.G., Habib, S., Messinger, D., Maltese, A. (Eds.), pp. 85380A. https://doi.org/10.1117/12.974857.
Walker, W.S., Stickler, C.M., Kellndorfer, J.M., Kirsch, K.M., Nepstad, D.C., 2010. Large-area classification and mapping of forest and land cover in the Brazilian amazon: A comparative analysis of ALOS/PALSAR and Landsat data sources. IEEE J. Sel. Top. Appl. Earth Obs. Remote Sens. 3, 594–604. https://doi.org/10.1109/JSTARS.2010.2076398.
Wang, X., Dong, X., Liu, H., Wei, H., Fan, W., Lu, N., Xu, Z., Ren, J., Xing, K., 2017. Linking land use change, ecosystem services and human well-being: A case study of the Manas River Basin of Xinjiang, China. Ecosyst. Serv. 27, 113–123. https://doi.org/10.1016/j.ecoser.2017.08.013.
Yengoh, G.T., Dent, D., Olsson, L., Tengberg, A.E., Tucker III, C.J., 2015. Use of the Normalized Difference Vegetation Index (NDVI) to Assess Land Degradation at Multiple Scales, SpringerBriefs in Environmental Science. Springer International Publishing, Cham. https://doi.org/10.1007/978-3-319-24112-8.
Yu, W., Zhou, W., Qian, Y., Yan, J., 2016. A new approach for land cover classification and change analysis: Integrating backdating and an object-based method. Remote Sens. Environ. 177, 37–47. https://doi.org/10.1016/j.rse.2016.02.030.
Zhu, X.X., Tuia, D., Mou, L., Xia, G.S., Zhang, L., Xu, F., Fraundorfer, F., 2017. Deep learning in remote sensing: A comprehensive review and list of resources. IEEE Geosci. Remote Sens. Mag. https://doi.org/10.1109/MGRS.2017.2762307.